Chapter IV

Experimental Results and Discussions:

4.1 Introduction:

The results of various experimental works explained in chapter III is compiled in this chapter. Section 4.2 gives the XRD results of crystalline-Si, crystalline-Ge, and a-Si:H. The results of electrical characterization of crystalline-Si and Ge is given in section 4.3. Section 4.3.1 gives the dc-electrical characterization of a-Si:H of the as prepared sample and samples annealed at various temperatures. The results of Fourier Transform Infra-red Spectroscopy of the crystalline-Si and Crystalline-Ge and also the as prepared a-Si:H is given in section 4.4. The Optical Transmission Spectrum of the crystalline silicon is presented in section 4.5 while the optical results of a-Si:H, for the as prepared as well as the annealed samples are presented in section 4.5.1.

4.2 XRD Results:

The X-ray diffractograms of crystalline-Si and crystalline-Ge are given in figures 4.1 and 4.2 respectively. The peaks correspond to <111> plane orientation. Both the samples were scanned in the range of $10°<2\theta<110°$. In the case of crystalline-Si a prominent single peak is observed at $2\theta = 69°53'$. For crystalline-Ge a prominent single crystal peak was observed at $2\theta = 28°39'$. These peaks corresponds to the <111> plane for both these samples. The significantly sharp peaks of the X-ray diffractograms establish the fact that the semiconductors are crystalline in nature. The X-ray diffractogram of the thin film a-Si:H does not show any prominent peaks,

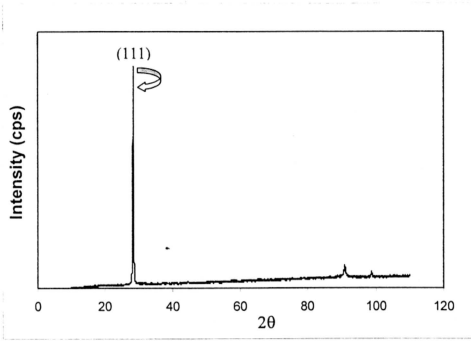

Figure 4.1 X-ray diffractogram of crystalline-Ge

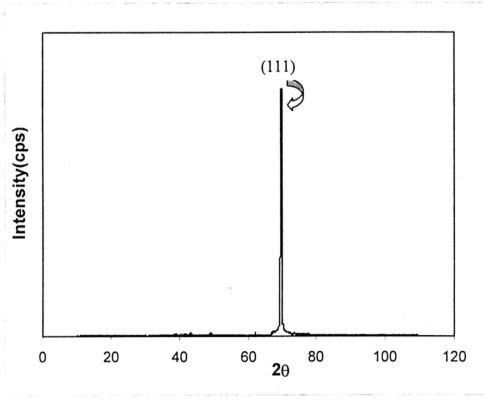

Figure 4.2 X-ray diffractogram of crystalline-Si

which confirms that the sample is amorphous. Figure 4.3 (a) is the spectrum of the a-si:H sample annealed at 500°C scanned in the range of 20° to 80°. The spectrum shows three peaks. The three peaks are seen at 2θ values of 22.01°, 38.32°, and 44.48° The first peak correspond to diffraction from (101) plane of silicon oxide (cristobalite) of tetragonal phase, the second peak correspond to diffraction from (302) plane of silicon of tetragonal phase while the third peak remained undetermined [56]. The sample has undergone recrystallization and has become polycrystalline after annealing at 500°C. A measure of the coherence length of the periodic structural pattern corresponding to a particular peak can be obtained from the full width at half-maximum through the Scherrer formula.[57].

$$L = \frac{0.9\lambda}{\Delta(2\theta)Cos(\theta_0)} \qquad (4.1)$$

Where L is the Scherrer or coherence length, λ is the wavelength of X-ray diffraction, θ_0 is the angle of reflection of the peak, and Δ(2θ) is the full width at half-maximum (FWHM).The grain size of the polycrystalline sample was computed through the Scherrer length using the formula [57]

$$D=4/3L. \qquad (4.2)$$

Where D is the spherical diameter of the grain. The grain size corresponding to the peak of maximum intensity corresponding to the Bragg reflected plane (302) was computed to be equal to 168.2nm. A representative figure used for the computation of the grain size for the maximum intensity is given in figure 4.3(b). For samples annealed at 100°C, 200°C, 300°C and 400°C, no prominent peaks were observed in the diffractogram.

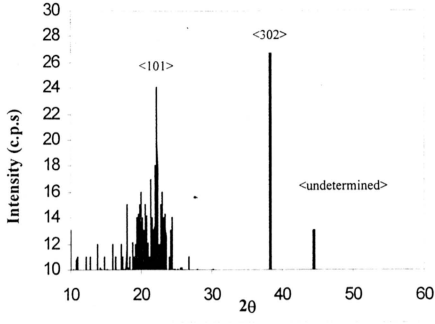

Figure 4.3(a) The X-ray diffractogram of a-Si:H

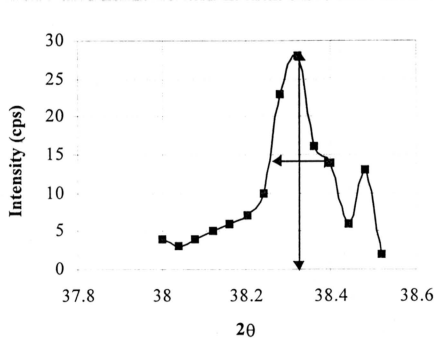

Figure 4.3 (b) Magnified peak of annealed a-Si:H with maximum intensity for the calculation of grain size.

4.3 Electrical results of crystalline semiconductors:

The lnσ Vs 1/T relationship of crystalline-Ge was studied using the Four-Probe technique, where σ is the conductivity and T is the measurement temperature. The temperature was increased from room temperature to 160°C. The variation of conductivity with increase in temperature is calculated and a graph of lnσ Vs 1/T was plotted which is given in figure 4.4. In the next chapter, the value of energy gap is derived from this result. Conductivity of crystal silicon was also measured by depositing aluminum electrodes in the transverse configuration on the sample and the measurements were carried out using Keithley Source measurement unit, as explained in chapter III. The temperature of the sample was increased from 300°K-475°K. The variation of lnσ with inverse temperature was studied and the

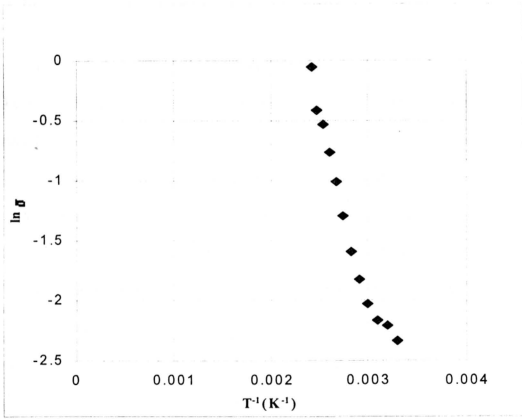

Figure 4.4 The variation of lnσ verses Temperature Inverse for crystalline-Ge

corresponding graph is given in figure 4.5.

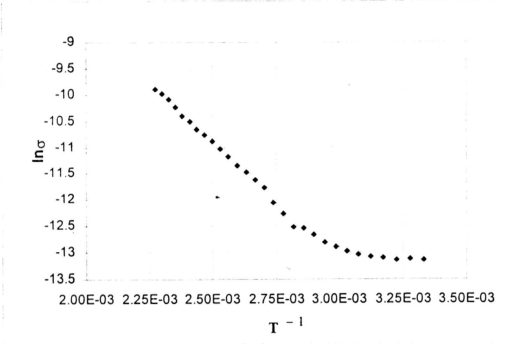

Figure 4.5 The variation of lnσ verses Temperature Inverse for crystalline-Si

4.3.1 Direct-Current Electrical Characterization of a-Si:H:

D.C Conductivity measurements were carried out on the as prepared as well as the annealed a-Si:H sample. The Current-Voltage characteristics at room temperature of the as prepared sample as well as the sample annealed at various annealing temperatures were studied in the presence and absence of light. Figure 4.6 and 4.7 depicts the current-voltage characteristic at room temperature of the As prepared and the sample annealed at different annealing temperatures in the presence of light and absence of light respectively. The sample was annealed at 100°C, 200°C, 300°C, 400°C and 500°C. From figures 4.6 and 4.7 it is evident that in the case of I-V measurements in the presence of light, the gradient is highest for the sample annealed at 400°C followed by the As prepared sample. The gradient is approximately the same for the other samples. A similar trend was observed in the

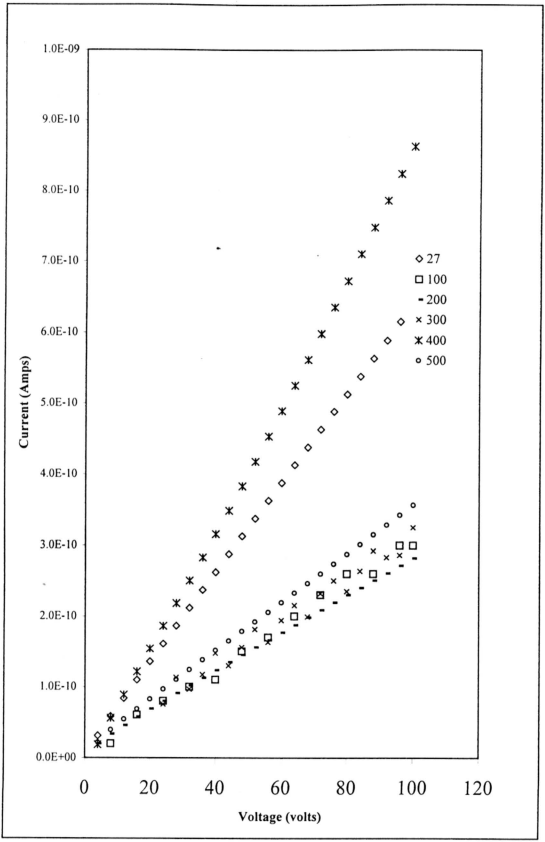

Figure 4.6 The Current verses Voltage graph for the As prepared sample and the sample annealed at various annealing temperatures in the presence of light at room temperature

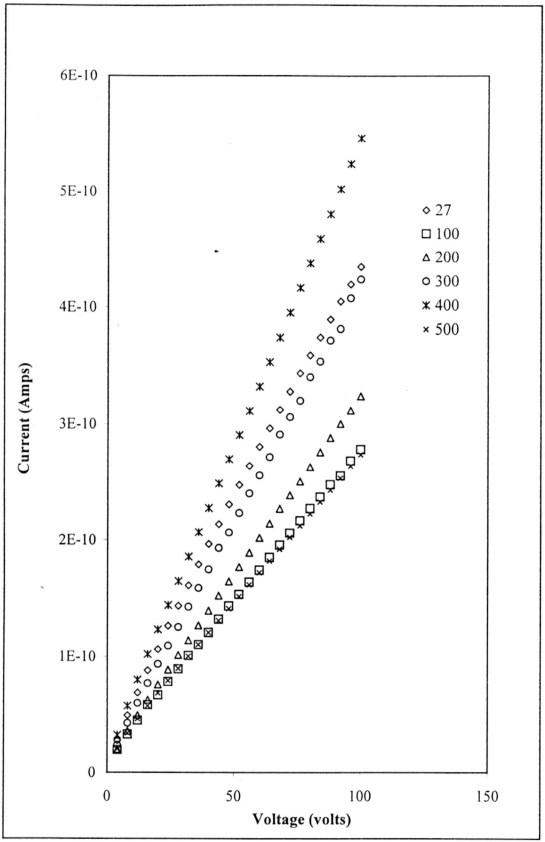

Figure 4.7 The Current verses Voltage graph for the As prepared sample and the sample annealed at various annealing temperatures in the absence of light at room temperature

I-V measurements of the sample in the absence of light. However the distinction in the gradient was not much prominent when compared to the measurements carried out in the presence of light. Then conductivity measurements were carried out after each annealing process. The conductivity measurements were carried out as mentioned in the Chapter III. The ln σ Vs 1000/T graphs obtained for the as prepared as well as the sample annealed at 100°C, 200°C, 300°C, 400°C and 500°C are plotted in the figure 4.8. It is evident from the figure that the hopping conductivity is prominent in all the samples in the low temperature region. The conductivity is highest for the sample annealed at 200°C and lowest for the sample annealed at 500°C. However the extended state conductivity was found to be highest in the sample annealed at 400°C. In the case of samples annealed at 400°C and 500°C, the sample is more ordered and has less localized state which resulted in a decrease in hopping conductivity. An abnormal trend is observed in the sample annealed at 100°C, where the conductivity increase with decrease in temperature in the low temperature regime between 200°K and 130°K which was quite difficult to understand within the framework of this work. From the figure 4.8 the activation energy in the three different states pertaining to the three different slopes for each sample, were calculated and the results are tabulated in Chapter V. A plot of $\ln(\sigma\sqrt{T})$ verses $\frac{1000}{T^{\frac{1}{4}}}$ for the as prepared and annealed samples are given in figure 4.9. It is seen that all the samples exhibit two linear regions, one in the high temperature region and the other in the low temperature region with the exception of the sample annealed at 100°C, which exhibited a linear trend only in the high temperature regime. The linear regions portrayed that Mott's variable range of hopping conductivity was prominent in all the samples. From the slope of the linear part of

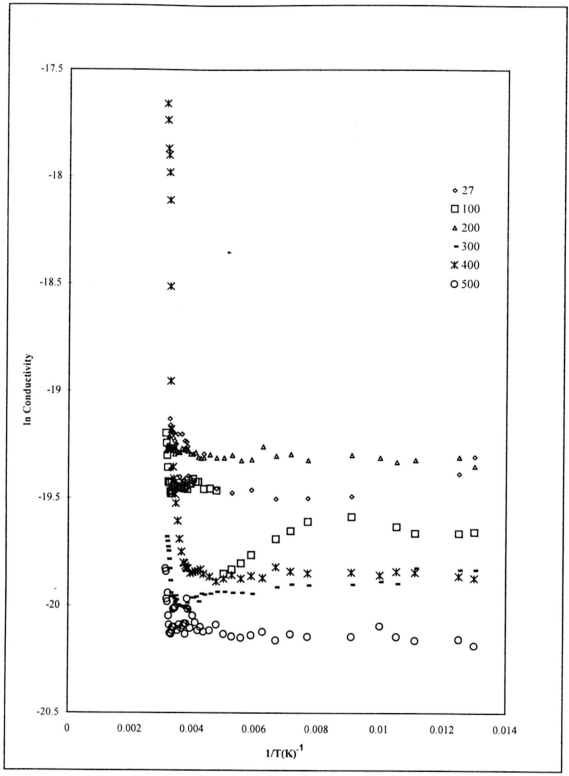

Figure 4.8 The variation of lns against Temperature Inverse for the As prepared sample and the sample annealed at various annealing temperatures

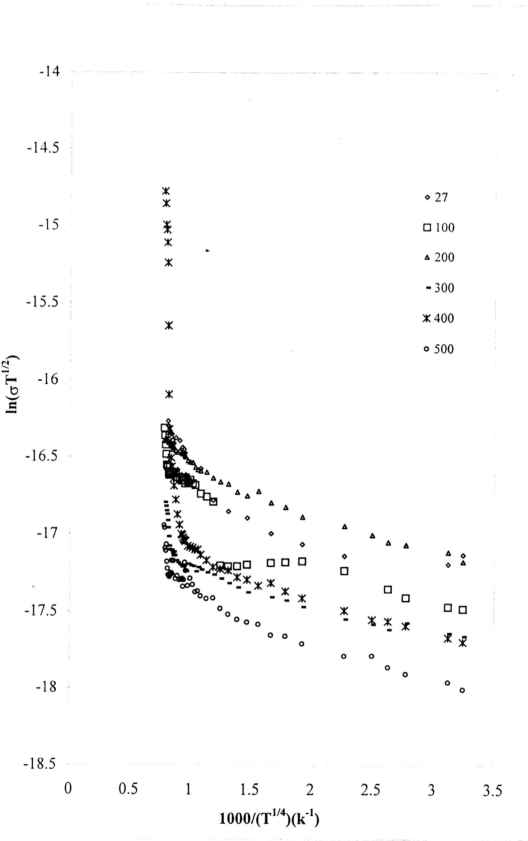

Figure 4.9 The T-Quarter relationship for the As prepared and the sample annealed at various annealing temperatures.

the figure 4.9 for each sample the density of the states at the Fermi level were calculated and the results are discussed in Chapter V.

4.4 Fourier Transform Infra-red Spectroscopy:

The Fourier Transform Infrared spectrum was taken for both crystalline and amorphous semiconductors. The main purpose of which is to ascertain the chemical bonding present in the sample. The infrared spectrum of crystalline-Ge is given in figure 4.10 and that of crystalline-Si is given in Figure 4.11. The transmission Spectrum of the crystalline semiconductors in the infrared region shows that the transmittance intensity decreases with increasing wave number. The spectrum of crystalline germanium shows two prominent valleys at wave numbers 575cm^{-1} and

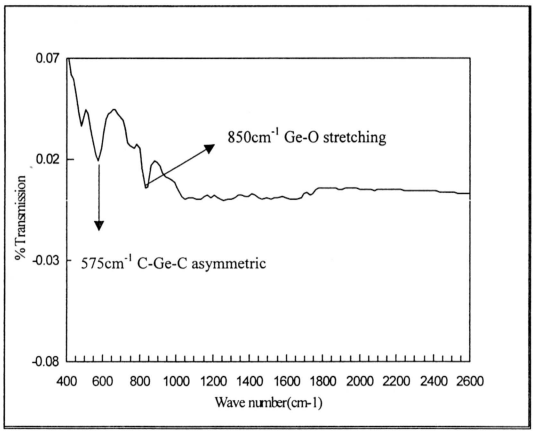

Fig: 4.10 The FT-IR spectrum of crystalline-Ge

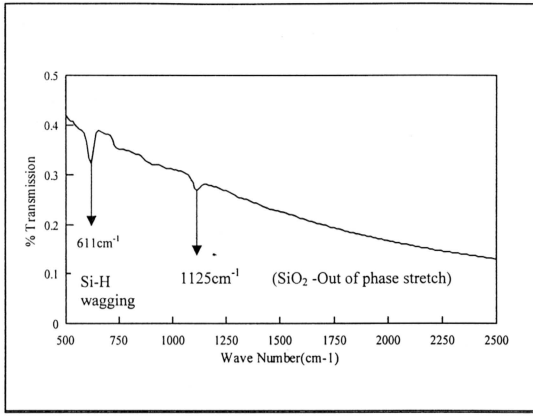

Figure 4.11 The FT-IR spectrum of crystalline-Si

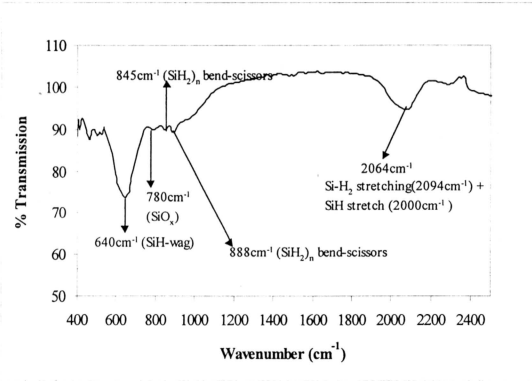

Figure 4.12 The FT-IR spectrum of a-Si:H

850cm^{-1} respectively which correspond to C-Ge-C asymmetric stretching [58,59] and Ge-O stretching band respectively [58,60,61]. while that of silicon shows two prominent dips at 611cm^{-1} and 1125cm^{-1} and they correspond to Si-H wagging [62,63,64] and SiO_2 stretching bonding [65]configurations respectively. The infrared spectrum of a-Si:H is given in figure 4.14. The spectrum shows that the transmittance intensity increases with increasing wave number. The spectrum exhibits two prominent troughs at 640cm^{-1} and 2064cm^{-1}. These troughs correspond to Si-H wagging [62-64] and Si-H_2 stretching [62,63,66] modes respectively. The spectrum also exhibits small troughs at 780cm^{-1}, which correspond to (SiO_X) [65,67-68], and the troughs at 845cm^{-1}, 888cm^{-1} correspond to (SiH_2)$_n$ bend scissors bonding configurations [64,69-73]

4.5 UV-VIS Optical Transmission Spectroscopy:

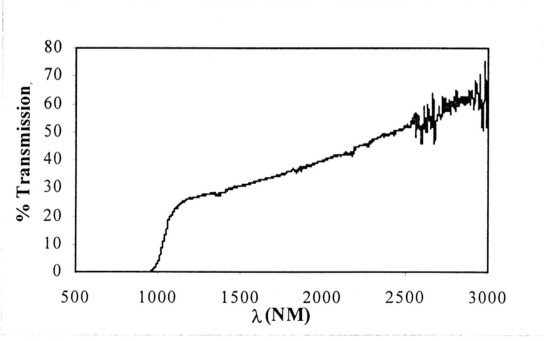

Figure 4.13 The UV-VIS optical transmission spectrum of crystalline-Si

The transmission spectrum of crystalline-Si was obtained by scanning the sample in

the range of 200nm-3000nm using the Shimadzu UV-VIS double beam spectrophotometer model. The spectrum obtained is given in figure 4.13. The spectrum shows that the % transmission decreases as the wavelength decreases. It is clearly observed that the fall of % transmission is sharp at about $964cm^{-1}$ whereas the fall of % transmission in the case of amorphous semiconductors is gradual which is evident from figures 4.14-4.19. From the transmission spectrum the refractive index, absorption coefficient and absorption constant were calculated as already explained in chapter II and the results are computed in chapter V.

4.5.1 Optical Results Of a-Si:H

The Optical transmission spectrum of the as prepared and also the annealed samples were obtained by using the JASCO UV-VIS double beam spectrophotometer model PC-310 by scanning the sample in the range of 200nm-2500nm. From these spectrum various optical properties of the thin film sample are analysed and discussed in Chapter V.The intensity of the peaks and the persence of interference fringes are characteristic of the thickness and the refractiveindex of the thin film. Thus we see the disappearance of the peaks when the film becomes denser and thinner as the film is annealed. The Optical spectrum of the as prepared and the annealed sample are given in figures 4.14, 4.15, 4.16, 4.17, 4.18, 4.19 below for comparison. Here, it is essential to mention that the same as prepared sample was annealed at different temperature and the optical spectrum of the sample was taken after each annealing temperature so that the effect of annealing on the sample can be studied. The intensity of the peaks decreases as the sample is annealed. It is also observed that the smallest peak shrink into a shoulder when the sample is annealed at 500°C. These results indicate that the thickness and refractive index changes when

the samples are annealed. The spectra were then analysed to calculate the refractive index, thickness of the film, absorption coeficient and hyrogen content in the sample, which are detailed in Chapter V.

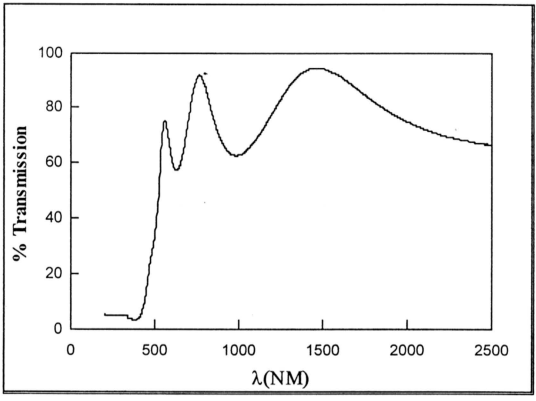

Figure 4.14The Optical Transmission Spectrum of the As Prepared Sample

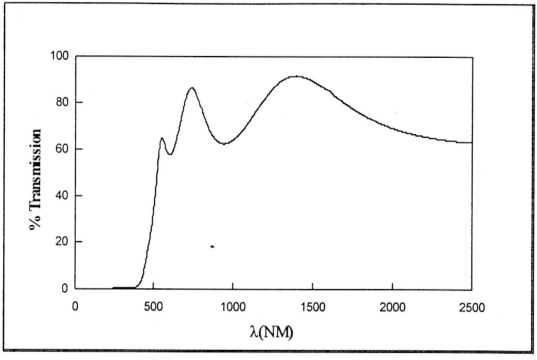

Figure 4.15 The Optical Transmission Spectrum of the sample annealed at 100°C

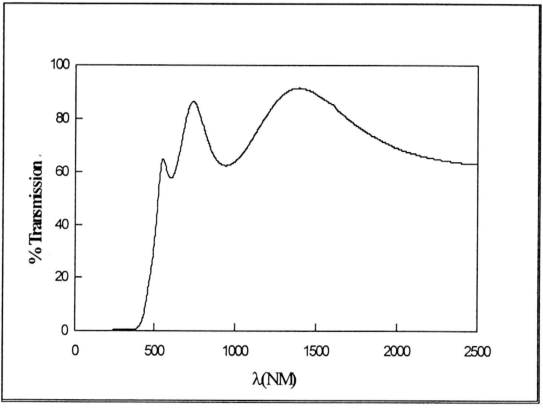

Figure 4.16 The Optical Transmission Spectrum of the sample annealed at 200°C

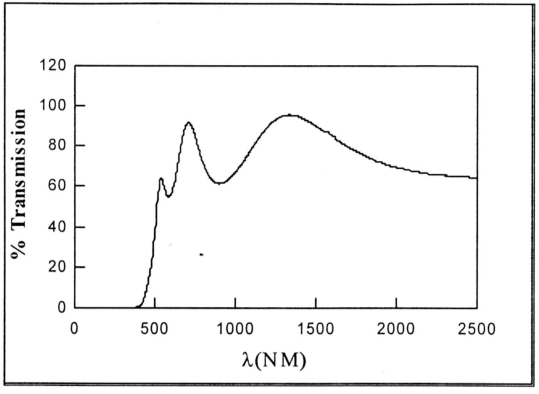

Figure4.17 The Optical Transmission Spectrum of the sample annealed at 300°C

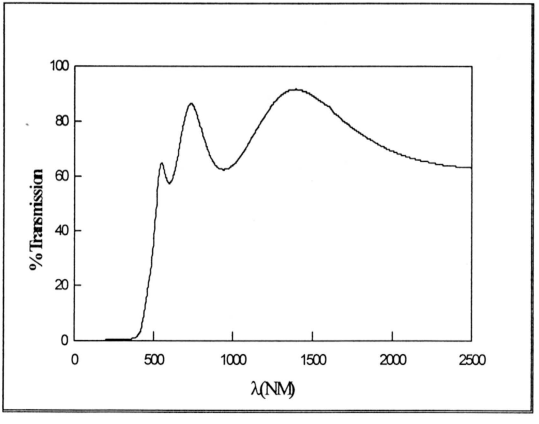

Figure 4.18 The Optical Transmission Spectrum of the sample annealed at 400°C

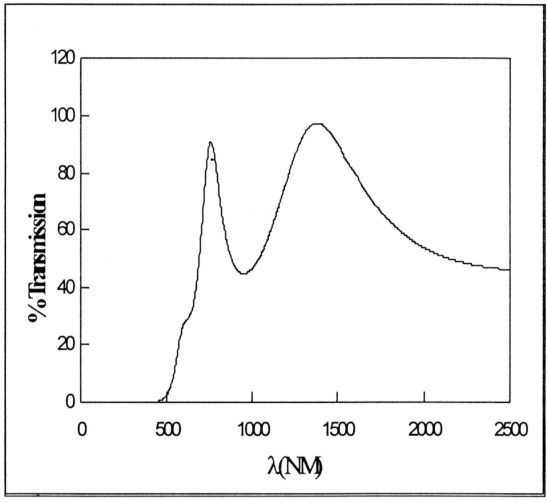

Figure 4.19 The Optical Transmission Spectrum of the sample annealed at 500°C